J Comput Aided Mol Des (2013) 27:951–964
DOI 10.1007/s10822-013-9692-0

Antioxidant properties of phenolic Schiff bases: structure–activity relationship and mechanism of action

El Hassane Anouar · Salwa Raweh · Imene Bayach · Muhammad Taha · Mohd Syukri Baharudin · Florent Di Meo · Mizaton Hazizul Hasan · Aishah Adam · Nor Hadiani Ismail · Jean-Frédéric F. Weber · Patrick Trouillas

Received: 12 October 2013 / Accepted: 9 November 2013 / Published online: 16 November 2013

Abstract Phenolic Schiff bases are known for their diverse biological activities and ability to scavenge free radicals. To elucidate (1) the structure–antioxidant activity relationship of a series of thirty synthetic derivatives of 2-methoxybezohydrazide phenolic Schiff bases and (2) to determine the major mechanism involved in free radical scavenging, we used density functional theory calculations (B3P86/6-31+(d,p)) within polarizable continuum model. The results showed the importance of the bond dissociation enthalpies (BDEs) related to the first and second (BDE_d) hydrogen atom transfer (intrinsic parameters) for rationalizing the antioxidant activity. In addition to the number of OH groups, the presence of a bromine substituent plays an interesting role in modulating the antioxidant activity. Theoretical thermodynamic and kinetic studies demonstrated that the free radical scavenging by these Schiff bases mainly proceeds through proton-coupled electron transfer rather than sequential proton loss electron transfer, the latter mechanism being only feasible at relatively high pH.

Keywords Schiff bases · Antioxidant · DFT · Kinetics · Free radical scavenging · BDE · Structure–activity relationship

Introduction

Natural and synthetic phenols including flavonoids, phenolic acids, stilbenoids and curcuminoids have been described as powerful antioxidants, being able to efficiently scavenge free radicals [1–3]. Schiff bases form an important class of synthetic phenolic compounds, substituted by a hydrazone

Electronic supplementary material The online version of this article (doi:10.1007/s10822-013-9692-0) contains supplementary material, which is available to authorized users.

E. H. Anouar (✉) · S. Raweh · I. Bayach · M. Taha · M. S. Baharudin · N. H. Ismail · J.-F. F. Weber
Atta-ur-Rahman Institute for Natural Product Discovery (RiND), Universiti Teknologi MARA, Kampus Puncak Alam, 42300 Bandar Puncak Alam, Shah Alam, Selangor DE, Malaysia
e-mail: anouarelhassane@yahoo.fr

S. Raweh · M. H. Hasan · A. Adam · J.-F. F. Weber
Faculty of Pharmacy, Universiti Teknologi MARA, Puncak Alam Campus, Shah Alam, Malaysia

I. Bayach
LCSN-Faculté de Pharmacie, Université de Limoges, 2 rue du Dr Marcland, 87000 Limoges, France

F. Di Meo · P. Trouillas (✉)
INSERM, UMR-S850/Faculté de Pharmacie, Université de Limoges, 2 rue du Dr Marcland, 87000 Limoges, France
e-mail: patrick.trouillas@unilim.fr

N. H. Ismail
Faculty of Applied Sciences, Universiti Teknologi MARA, 40450 Shah Alam, Malaysia

P. Trouillas
Laboratoire de Chimie des Matériaux Nouveaux, Université de Mons, Place du Parc, 20, 7000 Mons, Belgium

P. Trouillas
Regional Center of Advanced Technologies and Materials, Department of Physical Chemistry, Faculty of Science, Palacký University, 17. Listopadu 1192/12, 77146 Olomouc, Czech Republic

moiety. They are known for their various fields of application including inorganic chemistry, biological and analytical chemistry [4, 5]. Several studies focused on their biological activities as antibacterial [6–9], anticancer [5], and antifungal activities [10, 11]. Recently, we reported the antileishmanial activity of the series of synthetic Schiff bases studied in the present work (Fig. 1) [12]. Schiff bases also showed potent antioxidant activity to scavenge free radicals. In two recent studies, we reported the antioxidant activity of acylhydrazide and 2,4,6-trichlorophenylhydrazine Schiff bases as DPPH radical and super oxide anion scavengers [13, 14]. Free radical scavenging capacity of (poly)phenols is generally attributed to the hydrogen atom lability of the OH groups attached to aromatic rings (Ar) [3, 15–17]; however in some other antioxidants, NH and SH groups may provide labile hydrogen [18–24]. Antioxidants (ArX–H) may scavenge free radicals ($R^{\cdot}$) by H atom transfer through one of the four mechanisms:

(i) Hydrogen atom transfer (HAT) and proton-coupled electron transfer (PCET)

$$ArX{-}H + R^{\cdot} \rightarrow ArX^{\cdot} + R{-}H \quad (1)$$

This is the direct HAT, which is purely governed by the homolytic bond dissociation enthalpy (BDE) of X–H; note that the lower the BDE, the more important the role of the corresponding XH group in the antioxidant activity. PCET is distinguished from the pure HAT as it involves several molecular orbitals in an H-bonding pre-reaction complex [25–28]. The proton transfer is coupled to the electron transfer that occurs from a lone pair of the antioxidant to the singly occupied molecular orbital (SOMO) of the free radical.

(ii) Electron Transfer–Proton Transfer (ET–PT) or Sequential ET–PT (SET–PT)

$$ArX{-}H + R^{\cdot} \rightarrow ArXH^{+\cdot} + R^{-} \rightarrow ArX^{\cdot} + R{-}H \quad (2)$$

The first step of this reaction leads to the formation of the radical cation $ArXH^{+\cdot}$, which easily undergoes heterolytic dissociation of X-H bond leading to the same final products than those yielded by PCET. The first step is mainly governed by the ionization potential (IP) of the antioxidant.

(iii) Sequential Proton-Loss-Electron-Transfer (SPLET)

$$ArX{-}H \rightarrow ArO^{-} + H^{+} \quad (3)$$

$$ArX^{-} + R^{\cdot} \rightarrow ArX^{\cdot} + R^{-} \quad (4)$$

$$R^{-} + H^{+} \rightarrow RH \quad (5)$$

In this mechanism, a proton is lost prior to electron transfer from the subsequent anion to the free radical. SPLET is strongly favoured under alkaline conditions, which may help in the proton loss of the first step [29, 30].

(iv) AF (Adduct Formation)

$$ArX{-}\mathbf{H} + R^{\cdot} \rightarrow [ArXH{-}R]^{\cdot} \rightarrow \text{metabolites or } ArX^{\cdot} + RH \quad (6)$$

This mechanism is relatively specific to $^{\cdot}OH$ free radicals. It has been observed in radiolytic solutions. The radical may add on double bonds and aromatic rings. This mechanism is not considered in this work. As often shown in the literature, intrinsic parameters including BDE, IP and electron transfer enthalpy rationalize free radical scavenging capacities [3, 15, 16, 31] as the thermodynamic balance of the first three mechanisms is the same ($\Delta G^{CPET} = \Delta G^{ET-PT} = \Delta G^{SPLET}$). However to tackle the mechanisms of action, kinetic parameters should be considered [3, 24, 29, 32–34].

In the present study, we elucidate the structure–antioxidant activity relationship for a series of 30 synthetic derivatives of 2-methoxybezohydrazide phenolic Schiff bases (Fig. 1). The Schiff bases differ from the nature of the R-(aromatic) moiety attached to the nitrogen atom engaged in the –N=C double bond (Fig. 1). The compounds can be subdivided into three classes, namely (1) compounds **1**–**25**, where the aromatic ring is a benzene substituted with different OH, OCH_3, halogen, $COOCH_3$ and NO_2 groups, (2) compounds **26**–**28**, in which R is an unsubstituted pyridine attached at the three different possible positions and (3) compounds **29**–**30**, in which R is an unsaturated five-membered ring containing one heteroatom. The positive or negative contributions of different descriptors (e.g., number and position of OH groups, BDE, double (BDEd), IP, spin density distribution, intramolecular hydrogen bonds, presence of electron donating or withdrawing groups, and structural parameters) have been examined. The elucidation of the mechanism of action is based on a combined experimental and theoretical approach. For the theoretical approach, transition state and Marcus–Levich–Jortner theories were used to evaluate atom (PCET mechanism) and electron transfer (SPLET mechanism), respectively.

Methodology

Experimental synthesis

The *N*-benzylidene-2-methoxybenzohydrazide phenolic derivatives were synthesized by refluxing mixtures of 2 mmol 2-methoxy-benzohydrazide and different aldehydes in methanol and in the presence of catalytical amount of acetic acid for 3 h, according to the previously described method [12]. The reaction progress was monitored by thin layer chromatography (TLC); after completion, the solvent was evaporated under vacuum to afford the crude products, which were further re-crystallized in

Fig. 1 Structures of the synthesized Schiff bases

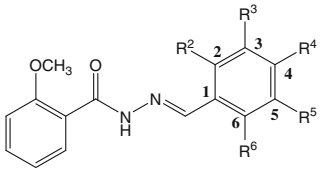

Monohydroxylated
1: $R^2 = OH$
2: $R^3 = OH$
3: $R^4 = OH$

Dihydroxylated
4: $R^2 = R^3 = OH$
5: $R^2 = R^4 = OH$
6: $R^2 = R^5 = OH$
7: $R^3 = R^4 = OH$
8: $R^3 = R^5 = OH$

Trihydroxylated
9: $R^2 = R^4 = R^6 = OH$
10: $R^3 = R^4 = R^5 = OH$

Monomethoxylated
11: $R^3 = OCH_3$
12: $R^4 = OCH_3$

Dimethoxylated
13: $R^3 = R^4 = OCH_3$
14: $R^3 = R^5 = OCH_3$

1-OH and 1-OCH$_3$
15: $R^2 = OH$, $R^4 = OCH_3$
16: $R^2 = OH$, $R^5 = OCH_3$
17: $R^3 = OH$, $R^4 = OCH_3$

Halogenated
18: $R^3 = Br$, $R^4 = OH$
19: $R^3 = Br$, $R^4 = Cl$
20: $R^4 = F$
21: $R^4 = Cl$
22: $R^2 = I$, $R^3 = OH$, $R^4 = OCH_3$

Other substitution
23: $R^4 = COOCH_3$
24: $R^4 = NO_2$

No substitution
25: $R^i = H$ (i = 2 to 6)

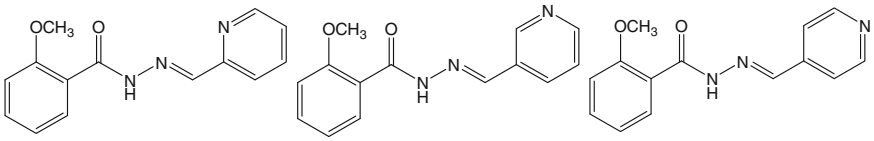

26 **27** **28**

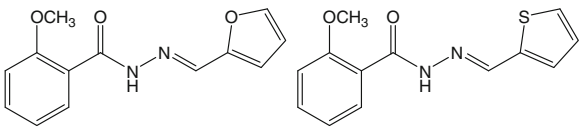

29 **30**

methanol. Needle-like pure products in good to excellent [0.40 g (78 %)–0.58 (92 %)] yields were obtained [12].

DPPH free radical scavenging capacity

The antioxidant capacity was evaluated as the capacity of the 30 different compounds to scavenge the 1,1-diphenyl-2-picrylhydrazil (DPPH) free radical, following the Blois' method [35]. The reaction mixture contains 5 μL of test sample (1 mM in DMSO) and 95 μL of DPPH (Sigma, 300 μM) in ethanol; it was placed into a 96-well microtiter plate and incubated at 37 °C for 30 min. The UV/Vis light absorbance was measured at 515 nm on microtiter plate reader (Molecular Devices, CA, and USA). The percentage of free radical scavenging was determined with respect to DMSO control. Following free radical scavenging versus compound concentration, IC_{50} was measured, which represent the concentration of compounds that scavenge 50 % of DPPH radicals (i.e., 50 % of absorbance at 515 nm). Propyl gallate was used as a positive control. All chemicals used were of analytical grade (Sigma, USA).

General computational details

Geometry optimization and frequency calculations have been carried out using density functional theory (DFT) as implemented in Gaussian09 [36]. To elucidate the structure–antioxidant activity relationship of polyphenols, the hybrid functional B3P86 appears reliable [15, 37, 38]. Increasing the number of polarization and diffuse functions have no significant effects on theoretical results, especially on BDEs and IPs [3, 15], therefore the calculations were performed with the 6-31+G(d,p) basis set. The ground states (GSs) geometries were confirmed by the absence of any imaginary frequency, while for the transition states (TSs) of PCET one imaginary frequency was obtained, which corresponds to H atom transfer. It has been shown that the B3P86 hybrid functional underestimates activation energy ($\Delta G^{\#}$) especially for hydrogen atom transfer reactions [29, 39]; in this course, MPWB1K appears more recommended even if overestimation are sometimes observed [40, 41]. The kinetic calculations of the PCET mechanism were performed with both (U)B3P86/6-31+G(d,p) and MPWB1K/6-31+G(d,p) methods.

Solvent effects were taken into account implicitly using the polarizable continuum model (PCM). In PCM models, the substrate is embedded into a shape-adapted cavity surrounded by a dielectric continuum characterized by its dielectric constant ($\varepsilon_{MeOH} = 32.613$) [42]. Using an explicit solvent were investigated by other authors [43], confirming that PCM succeeded in providing a reasonably accurate description of BDE, the main descriptor of antioxidant capacity. Hybrid models (i.e., one or two molecules in the surrounding of the OH groups + PCM) were also tested for quercetin, an antioxidant, showing only slight differences in terms of BDE when compared to pure PCM calculations, while computational time was dramatically increased [16].

Pre-reaction complexes, descriptions of non-covalent interactions and electron transfer kinetics

The rate constants of electron transfer (i.e., for ET–PT and SPLET mechanism) were evaluated within the Marcus–Levich–Jortner ($k^{LJ-Marcus}$) formalism according the following expression:

$$k^{LJ-Marcus} = \frac{4\pi^2}{h} \cdot V_{RP}^2 \sqrt{\frac{1}{4\pi\lambda_S k_b T}} \times \sum_{\upsilon'} \left\{ \frac{S^{\upsilon'}}{\upsilon'!} \cdot \exp(-S) \cdot \exp\left[-\frac{\left(\Delta G^\circ + \lambda_S + \upsilon' \hbar\omega\right)^2}{4\lambda_S k_b T} \right] \right\}$$

where ΔG° is the Gibbs energy difference of ET reactions (i.e., Eqs. (2) or (4) for SET–PT and SPLET, respectively), λ_S is the outer-shell reorganisation energy attributed to the solvent, V_{RP} is the electronic coupling, S is the Huang-Rhys factor and υ' is the vibrational quantum number. The sum runs over all effective vibrational modes, namely in our case aromatic C–C, phenolic C–O and C–N bond stretching. These bonds are the most probable reaction coordinates involved in electron transfer. ΔG°, λ_S, S were calculated following the previous study on free radical scavenging of quercetin [29]. V_{RP} was calculated from the pre-reaction complex geometries. They were calculated following the Farazdel et al. [44] approach with a Def2-TZVP basis set:

$$V_{RP} = \frac{H_{RP} - S_{RP}\frac{(E_R + E_P)}{2}}{1 - S_{RP}^2}$$

where H_{RP} is the total reactant–product interaction energy, S_{RP} is the reactant–product overlap, E_R and E_P are the electronic energies of reactants and products, respectively.

Pre-reaction complexes are of major importance in ET mechanisms since they drive the bimolecular mechanisms. These complexes involved either H-bond or [ν–π] dispersive interactions which are poorly described by classical hybrid functionals. Dispersion-corrected DFT-D is a successful approach to circumvent the use of expensive post-HF methods [45–47]. The B3P86-D2 functional was recently re-parameterized, reaching accuracy to evaluate dispersion effects in the non-covalent complexes involving natural polyphenols [48]. The geometries of the pre-reaction complexes were obtained at the B3P86-D2/Def2-TZVPP level of theory for all possible H-bond and [ν–π] complexes, i.e., either towards the OH groups or towards aromatic and N–N π-bonds. All calculations were carried out using Gaussian09 [36], Orca 2.8.1 [49] and NWCHEM 6.1.1 [50] packages for PCET, SPLET and electronic coupling calculations, respectively. When available, the RIJCOSX (resolution of identity and chain-of-sphere) approximations were used, allowing large speed-up of calculations for a minimal error [51].

Results and discussion

Experimentally-based (DPPH scavenging) structure–activity relationship

As usually observed for polyphenols, at least one phenolic OH group is required to provide an active compound (namely, **1–10**, **15–18**, **22** as seen in Table 1); the other compounds without OH group are inactive (namely, **11–14**, **19–21**, **23–30**). The position of OH groups is of crucial importance to modulate antioxidant capacity. Based on the measured IC_{50} values (Table 1), the active phenolic Schiff bases can be divided into three classes, depending on the number and position of the OH groups.

(i) One OH-group compounds (compounds **1–3**, IC_{50} ranging from 0.6 to 1.1 μg/mL)—In this case, compound **3** with a *para*-OH group is a stronger antioxidant than **1** having an *ortho*-OH group, being as well more active than **2** with a *meta*-OH group.

(ii) Two OH-group compounds (compounds **4–8**, IC_{50} ranging from 0.2 to 0.9 μg/mL)—The following order in terms of antioxidant activity is observed **7** ≈ **4** < **5** < **8** ≈ **6**. In the active phenolic Schiff bases **7** and **4**, the two OH groups are *ortho* to each other, which makes the compounds particularly active (IC_{50} about 0.2 μg/mL). This positive contribution of the catechol moiety is in agreement with the general literature on the structure–antioxidant activity relationship of polyphenols [1, 3, 15, 16]. Compound **5**, having two OH groups *meta* to each other, one being in *para* with respect to the N=C double bond is less active. Compounds **6** and **8**, having two OH groups *meta* to each other (no OH group at C4), are even much less active (Table 1). This highlights the importance of the *para* substitution in the benzene moiety.

Table 1 BDEs, IPs, spin density on the oxygen atom from which the hydrogen atom is removed, as obtained with PCM-B3P86/6-31+G (d,p), and experimental IC_{50} of the 30 Schiff bases

Schiff base	BDEd (Kcal/mol)						IP (eV)	Spin density[a]	IC_{50} (μg/mL)
	NH	2-OH	3-OH	4-OH	5-OH	6-OH			
1	96.5	83.8	–	–	–	–	6.4	0.27	0.90 ± 0.045
2	97.7	–	87.1	–	–	–	6.6	0.37	1.1 ± 0.05
3	95.7	–		83.2	–	–	6.3	0.32	0.65 ± 0.045
4	96.7	77.5	79.7		–	–	6.5	0.31	0.22 ± 0.045
5	94.7	82.4	–	82.2	–	–	6.2	0.25	0.34 ± 0.045
6	96.4	78.8	–		82.2	–	6.3	0.31	0.92 ± 0.045
7	95.8	–	78.8	76.1	–	–	6.2	0.25	0.20 ± 0.045
8	97.9	–	86.6		87.4	–	6.6	0.34	0.91 ± 0.0045
9	94.8	83.9	–	83.0	–	84.9	6.1	0.23	0.35 ± 0.045
10	95.7		80.2	72.3	81.68	–	6.2	0.27	0.30 ± 0.045
11	97.7	–	–	–	–	–	6.6	0.50	No activity
12	95.6	–	–	–	–	–	6.3	0.46	>>2
13	95.6	–	–	–	–	–	6.2	–	>>2
14	97.7	–	–	–	–	–	6.6	0.50	>>2
15	94.7	84.1	–	–	–	–	6.2	0.28	0.50 ± 0.071
16	97.2	79.2	–	–	–	–	6.2	0.31	1.01 ± 0.045
17	95.5		86.0	–	–	–	6.2	0.33	0.8 ± 0.002
18	96.6	–	–	82.2	–	–	6.4	0.26	0.22 ± 0.0045
19	99.0	–	–	–	–	–	6.7	0.53	>>2
20	97.4	–	–	–	–	–	6.6	0.49	>>2
21	97.7	–	–	–	–	–	6.6	0.49	>>2
22	–	–	–	–	–	–	–	–	1.63 ± 0.21
23	98.6	–	–	–	–	–	6.8	0.45	>>2
24	99.6	–	–	–	–	–	7.0	0.50	>>2
25	97.5	–	–	–	–	–	6.6	0.51	>>2
26	98.4	–	–	–	–	–	6.9	0.57	>>2
27	98.5	–	–	–	–	–	6.8	0.51	>>2
28	99.4	–	–	–	–	–	7.0	0.54	>>2
29	94.9	–	–	–	–	–	6.4	0.45	>>2
30	95.1	–	–	–	–	–	6.4	0.44	>>2

[a] Spin density of the active OH site

(iii) Three OH-group compounds (compounds **9**–**10**)—Compound **10** is a stronger antioxidant than **9**, is particularly due to the adjacent three OH groups.

The main trend observed here is that compounds of the first class are less active than those of the other two classes. Moreover the presence of two OH groups *ortho* to each other and one OH group *para* is of crucial importance to increase the activity. An additional third OH group is not mandatory to increase the antioxidant capacity, as already observed for myricetin with respect to quercetin [1].

Another interesting feature derived from this series of compounds concern the effect of bromination and methoxylation of phenolic ring. To emphasize this effect on the antioxidant activity, compound **7** (3-OH, 4-OH) is compared to both **17** (3-OH, 4-OCH_3), and **18** (3-Br, 4-OH). The methoxylation significantly reduces the antioxidant activity (Table 1), while interestingly the bromine at C3 makes compound **18** as active as **7** (having the active catechol moiety).

Theoretical rationalization

The free radical scavenging capacity has been extensively correlated to O–H BDEs, rationalized by spin density distribution and stability of the phenoxyl radical ($ArX^{\cdot}$ with X=O) formed after HAT. In principle, N–H BDE may also correlate with the free radical scavenging capacity, since the hydrogen of these groups may be labile according to the

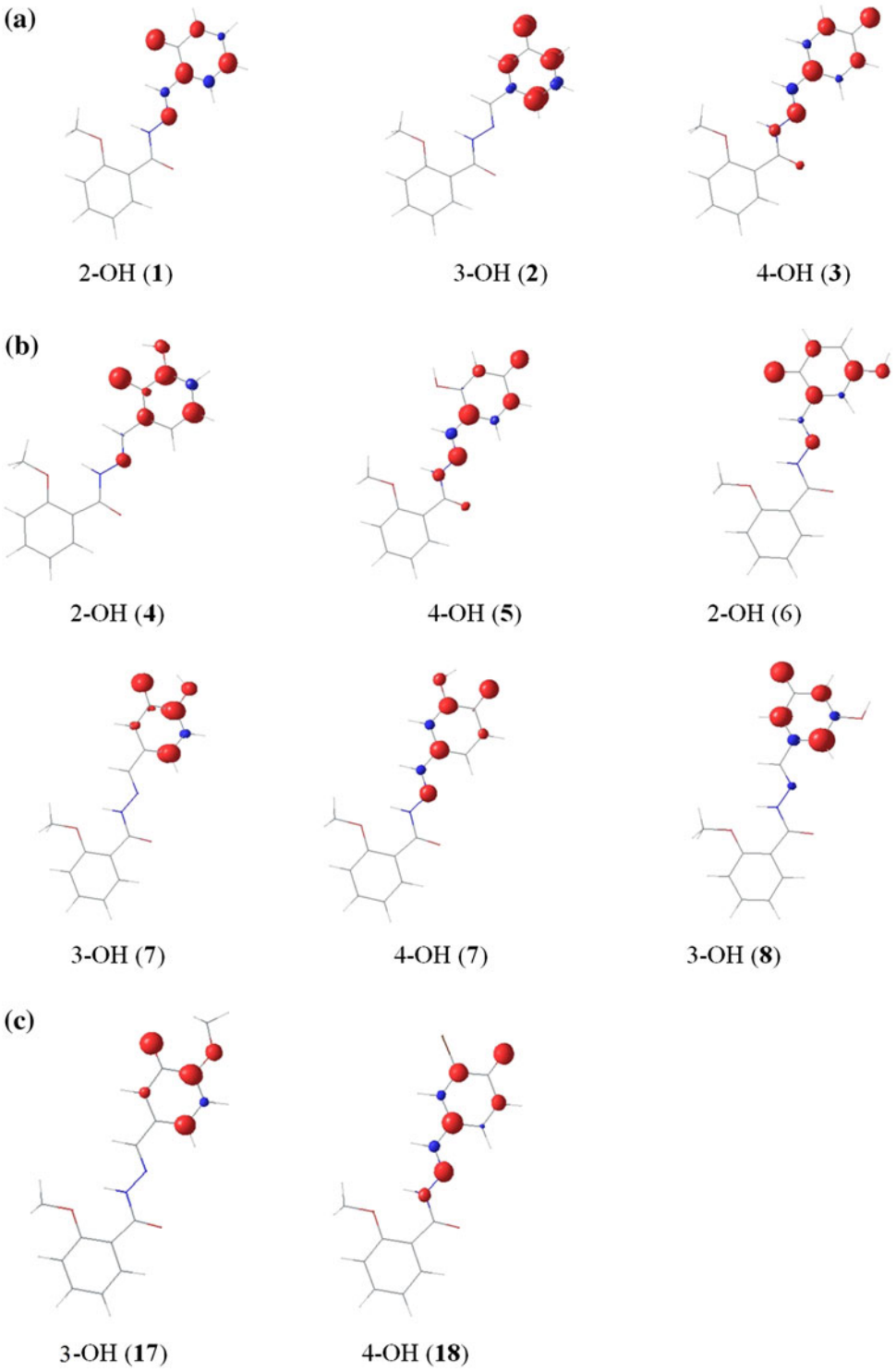

Fig. 2 Spin density distribution of the radicals obtained after first HAT transfer (**a**) 2-OH, 3-OH, 4-OH groups for compounds **1**, **2** and **3** (**b**) 2-OH, 4-OH, 2-OH, 4-OH and 3-OH groups for compounds **4**, **5**, **6**, **7** and **8** (**c**) 3-OH and 4-OH groups for compounds 17 and 18

chemical neighboring. The inactive compounds (**11**–**14**, **19**–**21**, **23**–**30**) having no OH group, and thus no O–H BDE, could have only been active due to the NH group. However all N–H BDEs of this series of compounds are higher than 90 kcal/mol (Table 1), making these compounds inefficient to scavenge DPPH. Indeed, the BDE of DPPH-H is ca. 80 kcal/mol [38, 52], thus for these compounds the thermodynamic balance of Eq. 1 is positive with DPPH.

In the first class of active compounds (**1**–**3**), the low antioxidant activity of **2** is in agreement with the relatively high BDE of the *ortho*-2-OH group (87.1 kcal/mol)

Table 2 BDE_d and IP_d of Schiff bases, as calculated with PCM-B3P86/6-31+G(d,p)

Schiff base	BDEd (Kcal/mol)							IC_{50} (μg/mL)
	NH	2-OH	3-OH	4-OH	5-OH	6-OH	IPd (eV)	
1-(2-OH)	88.7	–	–	–	–	–	6.5	0.90 ± 0.045
2-(3-OH)	112.1	–	–	–	–	–	7.1	1.1 ± 0.05
3-(4-OH)	86.1	–	–	–	–	–	6.4	0.65 ± 0.045
4-(2-OH)	91.8	–	76.7	–	–	–	6.5	0.22 ± 0.045
5-(4-OH)	84.9	94.1	–	–	–	–	6.4	0.34 ± 0.045
6-(2-OH)	90.7	–	–	–	68.8	–	6.2	0.92 ± 0.045
7-(4-OH)	87.3	–	75.9	–	–	–	6.2	0.20 ± 0.045
8-(3-OH)	113.3	–	–	–	107.9	–	7.1	0.91 ± 0.0045
9-(4-OH)	84.6	95.0	–	–	–	83.6	6.4	0.35 ± 0.045
10-(4-OH)	88.1	–	76.6	–	79.1	–	6.2	0.30 ± 0.045
15-(2-OH)	86.3	–	–	–	–	–	6.4	0.50 ± 0.071
16-(2-OH)	91.8	–	–	–	–	–	6.1	1.01 ± 0.045
17-(3-OH)	100.6	–	–	–	–	–	6.3	0.8 ± 0.002
18-(4-OH)	86.8	–	–	–	–	–	6.4	0.22 ± 0.0045
22-(3-OH)	–	–	–	–	–	–	–	1.63 ± 0.21

compared to those of the *meta*-3-OH and *para*-4-OH groups (83.8 and 83.1 kcal/mol, respectively). The BDE is related to the capacity of the phenoxy radical ($ArO^{\cdot}$) formed after HAT (Eq. 1) to stabilize by π-conjugation. The higher BDE obtained for the 2-OH group is attributed to a lower spin density delocalization in the corresponding $ArO^{\cdot}$ (Fig. 2a-middle) compare to the better π-conjugation observed when HAT occurs at 3-OH (Fig. 2a-left and right). Regarding both compounds **1** and **3**, the BDEs are similar (difference in BDE ca. 0.5 kcal/mol as seen in Table 1), while the latter compound is more active as free radical scavenger (Table 1). This shows that BDE cannot be the only descriptor to fully rationalize slight antioxidant activities. In this case, the spin density distribution better explain this difference i.e., $ArO^{\cdot}$ obtained after HAT from **3** exhibits a better electron delocalization (Fig. 2a-right). In next section this is even better rationalized with another secondary descriptor.

In the second class of active compounds (**4**–**8**), the role of the catechol moiety (compounds **4** and **7**) is rationalized by the low BDE values, namely 76.1 and 77.5 kcal/mol for 2-OH (**4**) and 4-OH (**7**), respectively. The low BDEs obtained in the catechol moiety is attributed to the stabilization of the corresponding $ArO^{\cdot}$ by spin delocalization (Fig. 2b) and intramolecular H-bonding. In compound **7**, the 4-OH group has a lower BDE (76.1 kcal/mol) than the 3-OH group (78.8 kcal/mol), in agreement with the better spin density delocalization when HAT occurs from the former group (Fig. 2b). Compare to **4** and **7**, the Schiff bases **5**, **6** and **8** exhibit higher BDEs, as correlated by the higher IC_{50} values (Table 1). This again exemplified the importance of the catechol moiety in the antioxidant activity.

In the third class, the Schiff base **10** is more active than **9**. This is attributed to the low BDE of 4-OH in **10** (72.3 kcal/mol) (Table 1).

The decrease in free radical scavenging capacity observed from **7** to **17** (after methylation of 4-OH) is simply attributed to the loss of the most active group [having the lowest BDE and no delocalization of spin density (Fig. 2c-left)]. When methylation occurs on the other OH groups, the effects on BDE is lower and the free radical scavenging capacity is not significantly reduced (Table 1).

The substitution of position 3 by a bromine (compound **18**) slightly decreases the 4-OH BDE compare to compound **3**, having only one OH group at C4 (Table 1) and increases spin delocalization in the related phenoxy radical compare to compound **7** (Fig. 2c-right). This agrees perfectly with a relatively good free radical scavenging capacity (Table 1), showing the role of bromine substitution in enhancing the antioxidant activity.

Double BDE analysis

The free radical scavenging capacity can be rationalized by HAT from one of the active OH group, but it has also been explained that a second HAT may occurs from active compounds (to scavenge a second free radical). This has been rationalized by the double BDE (BDE_d) descriptor. In case, the calculated BDEs have similar values, BDE_d may appear as an efficient descriptor to rationalize slight

Table 3 Gibbs energies of the HAT and ET processes (ΔG^{HAT} and ΔG^{ET}) of Schiff bases with the DPPH and $CH_3OO^{\cdot}$ free radical, as obtained with B3P86/6-31+G (d,p)

Schiff base	HAT mechanism				ET mechanism			
	ΔG^{HAT} with DPPH		ΔG^{HAT} with CH3OO$^{\cdot}$		ΔG^{ET} with DPPH		ΔG^{ET} with CH3OO$^{\cdot}$	
	Gas	Solvent	Gas	Solvent	Gas	Solvent	Gas	Solvent
(a) First HAT								
1	2.9	7.5	−1.6	−0.5	88.0	26.3	143.1	45.7
2	7.1	10.8	2.6	2.8	91.3	29.4	146.5	48.7
3	4.1	6.8	−0.4	−1.2	85.8	23.8	141.0	−1.2
4	−4.1	1.5	−8.6	−6.5	87.4	26.2	142.6	45.6
5	0.9	5.7	−3.5	−2.3	81.9	21.9	137.1	41.3
6	−1.3	2.3	−7.8	−5.6	85.4	24.1	140.5	43.5
7	−4.6	0.2	−9.1	−7.9	84.4	21.7	139.5	41.1
8	6.2	10.3	1.7	2.3	91.2	29.2	146.4	48.6
9	2.7	6.6	−1.8	−1.4	79.1	21.4	134.2	40.8
10	−8.1	−2.7	−12.6	−10.7	83.6	23.5	138.7	42.9
11	15.8	20.5	11.3	12.5	89.4	28.8	144.5	48.1
12	14.5	18.5	10.0	10.4	82.8	–	137.9	–
13	14.8	18.2	10.3	10.2	79.2	20.7	143.4	40.4
14	15.9	20.4	11.4	12.4	87.6	28.1	142.7	47.5
15	7.4	7.7	−0.7	−0.4	79.7	20.0	134.8	39.3
16	−1.2	0.0	−5.7	−8.0	83.5	21.0	138.6	40.4
17	5.4	9.3	0.8	1.3	81.3	20.1	136.4	39.4
18	14.9	6.0	10.5	−2.1	88.4	25.9	143.5	39.8
19	16.0	21.0	11.5	13.0	95.7	32.3	150.8	51.6
20	15.8	20.4	11.3	12.4	93.7	30.0	148.8	49.4
21	16.0	20.7	11.5	12.7	93.5	30.5	148.6	49.8
22	–	–	–	–	–	–	–	–
23	16.3	21.3	11.8	13.3	95.6	33.2	150.7	52.5
24	17.1	21.2	12.6	14.2	104.2	37.4	159.3	56.8
25	15.8	20.3	11.4	12.4	92.9	30.2	148.0	49.5
26	14.6	20.8	10.1	12.8	97.3	35.2	152.4	54.6
27	16.3	21.2	11.8	13.2	98.1	33.7	153.2	53.0
28	16.2	21.7	11.8	13.7	103.3	38.2	158.4	57.6
29	13.7	18.0	9.2	10.0	88.5	24.5	143.6	43.8
30	13.6	18.2	9.1	10.2	88.5	25.0	143.7	44.3
(b) Second HAT								
1	7.0	11.9	1.0	−1.6	91.8	28.0	146.9	42.0
2	33.5	35.2	27.5	21.7	106.9	42.5	161.9	56.5
3	10.2	9.4	4.2	−3.9	90.3	25.7	145.4	39.7
4	−0.4	−0.5	−6.4	−14.0	92.0	29.5	147.0	43.4
5	18.8	18.1	12.8	4.6	88.7	25.0	143.7	38.9
6	−12.5	−7.6	−18.5	−21.0	84.5	21.4	139.5	35.4
7	−0.8	−0.6	−6.8	−14.1	85.8	23.4	140.8	37.3
8	32.3	30.3	26.3	16.9	107.1	43.9	162.1	57.8
9	5.3	9.3	−0.8	−4.2	87.6	26.7	142.6	40.6
10	−0.5	0.1	−6.5	−13.4	85.3	21.2	140.3	35.2
15	5.5	9.7	−0.5	−3.7	88.7	27.5	143.7	41.5

Table 3 continued

Schiff base	HAT mechanism				ET mechanism			
	ΔG^{HAT} with DPPH		ΔG^{HAT} with CH3OO$^{\cdot}$		ΔG^{ET} with DPPH		ΔG^{ET} with CH3OO$^{\cdot}$	
	Gas	Solvent	Gas	Solvent	Gas	Solvent	Gas	Solvent
16	10.1	15.7	4.1	2.3	81.7	22.1	136.7	36.1
17	21.6	24.2	15.6	10.8	87.1	25.1	142.1	39.1
18	3.9	9.8	−2.1	−3.6	90.4	26.5	145.4	40.5

Table 4 Free energies of activation ($\Delta G^{\#}$) and rate constants (k^{TST}, $k^{TST/W}$ and $k^{TST/ST}$) of HAT mechanism of the active Schiff bases with the CH_3OO ($R^{\cdot}$) free radical, as obtained with hybrid functionals B3P86 and MPWB1K

No. of OH in aromatic ring	ArO-**H** + $R^{\cdot}$ → $ArO^{\cdot}$ + RH (ArO-**H** = 1–10)	$\Delta G^{\#}$	K^{TST}	$K^{TST/W}$	$K^{TST/ST}$
B3P86					
1-OH	**1**	12.26	6.5×10^{3}	2.9×10^{4}	6.5×10^{3}
	2	15.09	5.5×10	2.2×10^{2}	5.5×10
	3	11.99	1.0×10^{4}	5.2×10^{4}	1.0×10^{4}
2-OH	**4**	10.73	8.6×10^{4}	2.3×10^{5}	8.6×10^{4}
	5	11.47	2.5×10^{4}	1.2×10^{5}	2.5×10^{4}
	6	9.39	8.3×10^{5}	3.3×10^{6}	8.3×10^{5}
	7	8.82	2.2×10^{6}	9.3×10^{6}	2.2×10^{6}
	8	14.36	1.9×10^{2}	1.1×10^{3}	1.9×10^{2}
3-OH	**9**	11.55	2.2×10^{4}	1.0×10^{5}	2.2×10^{4}
	10	11.53	2.2×10^{4}	3.9×10^{4}	2.2×10^{4}
MPWB1K					
1-OH	**1**	22.44	2.3×10^{-4}	1.0×10^{-3}	2.3×10^{-4}
	2	23.76	2.5×10^{-5}	1.0×10^{-4}	2.5×10^{-5}
	3	23.20	6.4×10^{-5}	3.2×10^{-4}	6.4×10^{-5}
2-OH	**4**	22.00	4.8×10^{-4}	1.3×10^{-3}	4.8×10^{-4}
	5	22.26	3.1×10^{-4}	1.5×10^{-3}	3.1×10^{-4}
	6	17.97	4.3×10^{-1}	1.7×10	4.3×10^{-1}
	7	18.10	3.5×10^{-1}	1.5×10	3.5×10^{-1}
	8	24.16	1.3×10^{-5}	7.1×10^{-5}	1.3×10^{-5}
3-OH	**9**	21.09	2.2×10^{-3}	1.1×10^{-2}	2.2×10^{-3}
	10	20.02	1.4×10^{-2}	2.3×10^{-2}	1.4×10^{-2}

Table 5 Structural parameters of the transition state of active Schiff bases and the peroxyl CH3OO$^{\cdot}$ obtained with B3P86 functional

Schiff base	Distance (Å)				Angle (°)				Torsional angle (°)		
	C_a–O_a	O_a–H_a	H_a–O_r	O_r–O_r	C_a–O_a–H_a	O_a–H_a–O_r	H_a–O_r–O_r	O_r–O_r–C_r	C_a–O_a–H_a–O_r	O_a–H_a–O_r–O_r	C_a–O_a–O_r–O_r
1	1.302	1.181	1.204	1.378	120	169	105	110	180	−180	0
2	1.311	1.161	1.214	1.378	115	167	104	109	94	−102	−10
3	1.304	1.139	1.257	1.380	119	170	105	109	−179	179	0
4	–	–	–	–	–	–	–	–	–	–	–
5	1.305	1.127	1.275	1.381	119	170	106	109	−180	180	0
6	1.313	1.103	1.307	1.376	118	169	106	109	180	−180	0
7	1.314	1.110	1.295	1.370	118	171	106	109	−180	180	0

Table 5 continued

Schiff base	Distance (Å)				Angle (°)				Torsional angle (°)		
	C_a–O_a	O_a–H_a	H_a–O_r	O_r–O_r	C_a–O_a–H_a	O_a–H_a–O_r	H_a–O_r–O_r	O_r–O_r–C_r	C_a–O_a–H_a–O_r	O_a–H_a–O_r–O_r	C_a–O_a–O_r–O_r
8	1.304	1.173	1.212	1.380	120	170	105	109	167	−170	−3
9	1.305	1.126	1.278	1.382	118	170	106	109	−178	178	0
10	–	–	–	–	–	–	–	–	–	–	–

a: refers to the atom of antioxidant, r: refers to atom of peroxyl radical

Table 6 Relative energy stabilization (ΔE) of both studied anion **7**-[3H+] and **7**-[4H+], internal λ_i and external λ_s reorganization energies (kcal mol^{-1}), electronic coupling V_{RP} (kcal mol^{-1}), Gibbs energy of the reaction ΔG° (kcal mol^{-1}), SPLET rate constants k (M^{-1} s^{-1}) for all H-bond and [***ν*–*π***] complexes

Anion	ΔE	Conformation	λ_i	λ_s	V_{RP}	ΔG°	k^{SPLET}
7-[3H+]	0.00	$[\nu–\pi]_{Abot}$	14.78	20.22	0.12	21.96	1.4×10^{-6}
		$[\nu–\pi]_{Atop}$	14.78	14.30	1.53	21.89	5.6×10^{-5}
		$[\nu–\pi]_{Bbot}$	14.78	4.31	1.45	21.53	3.0×10^{-17}
		$[\nu–\pi]_{Btop}$	14.78	2.70	0.27	21.70	1.5×10^{-30}
		[HB-4]	14.78	14.32	1.54	22.01	5.7×10^{-5}
7-[4H+]	−2.60	$[\nu–\pi]_{Abot}$	14.08	18.33	3.71	21.90	1.7×10^{-3}
		$[\nu–\pi]_{Atop}$	14.08	25.00	4.61	21.83	2.6×10^{-3}
		$[\nu–\pi]_{Bbot}$	14.08	7.29	3.90	22.18	1.9×10^{-8}
		$[\nu–\pi]_{Btop}$	14.08	14.61	1.50	21.68	9.3×10^{-5}
		[HB-3]	14.08	13.85	0.43	21.98	5.2×10^{-6}

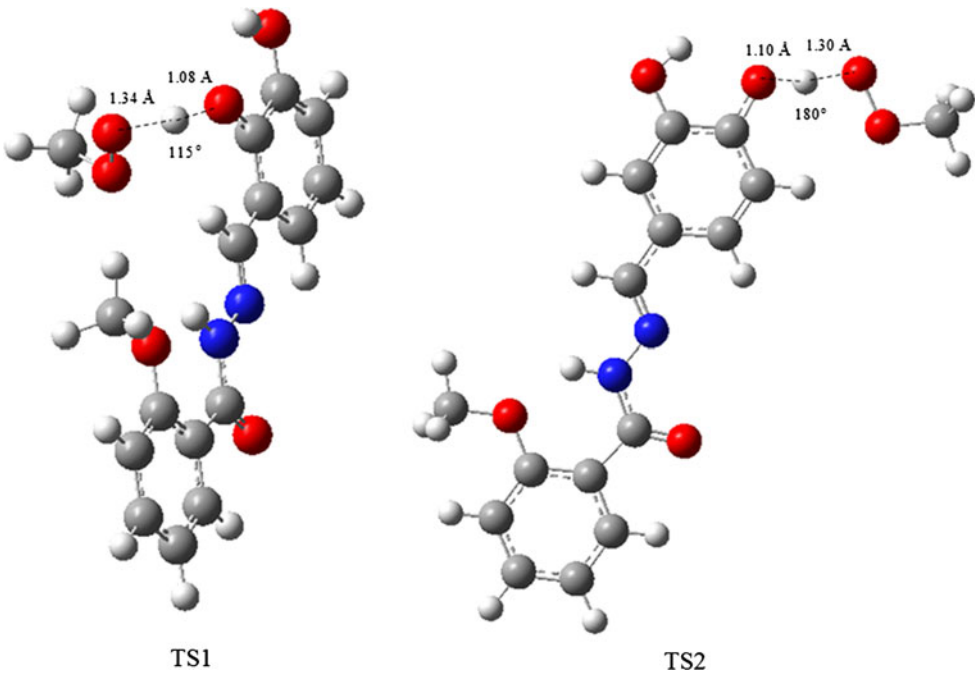

Fig. 3 Geometries of the PCET transition states between the Schiff bases **4** (*left*) and **7** (*right*), and the peroxyl radical $CH_3OO^{\cdot}$

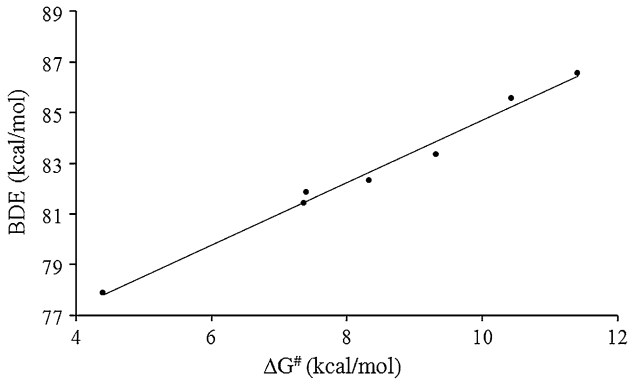

Fig. 4 Correlation between BDE and free activation energy ($\Delta G^{\#}$) for peroxyl radical scavenging by active Schiff bases (**1**–**10**)

variations of the antioxidant activity. BDE_d appeared particularly adequate to differentiate the antioxidant activity of a series of synthetic oligomers of guaiacol [3]. BDE_d values of the second and third classes (two and three OH groups, respectively) of Schiff bases are reported in Table 2. To highlight the potent role of this descriptor, compounds **8** and **17** were considered. After HAT from 20-OH (having very similar BDEs in both compounds), the BDE_ds from the NH group are 113.3 and 100.6 kcal/mol (Table 2), respectively, which agrees with the better activity for the latter compound. Another example concerns compounds **1** and **3**, for which the O–H BDEs are very similar (difference lower than 0.6 kcal/mol, as seen in Table 1) while the N–H BDE_d difference is 2.6 kcal/mol in favor of compound **3** (Table 2), in agreement with the better antioxidant activity of **3** (Table 3).

Mechanism of free radical scavenging

The capacity of antioxidant to scavenge free radicals depends on intrinsic parameters as BDE but also on the nature of the free radical itself. In terms of thermodynamics, the radical scavenging depends on the Gibbs energy of Eq. 1. Here we focus on DPPH and a prototype of peroxy radical ($CH_3OO^{\cdot}$). The free radical scavenging of DPPH usually correlate relatively well with that of peroxy radicals even if both radicals are chemically different [31]. The thermodynamic balance is calculated for both reactions:

$$\mathrm{ArO{-}\mathbf{H} + DPPH^{\cdot} \rightarrow ArO^{\cdot} + DPPH{-}\mathbf{H}} \quad (1')$$

$$\mathrm{ArO{-}\mathbf{H} + CH_3OO^{\cdot} \rightarrow ArO^{\cdot} + CH_3OO{-}\mathbf{H}} \quad (1'')$$

In order to tackle the mechanism of action of free radical scavenging, the kinetics of the limiting step should be evaluated. Here only the kinetics of $CH_3OO^{\cdot}$ scavenging was evaluated. Regarding the large Gibbs energy of the ET step in the SET–PT process (higher than 40 kcal/mol as seen in Table 4), this mechanism appears unlikely, as usually described in the literature [3]. The competition may occur between PCET and SPLET.

The former mechanism is described by the transition state theory. Tables 5 and 6 report the rate constants, Gibbs energies of activation and structural parameters of transition states (distance, angles and torsion angles). In the transition state, the hydrogen atom is approximately located between the phenoxyl and peroxyl radicals (Fig. 3).

As explained above the B3P86 hybrid functional underestimates Gibbs energy of activation, while MPWB1K give a better description of PCET [29, 39]. Therefore the values reported in Table 5 only provide a range. In this process, tunneling appears crucial thus rate constants are more relevant than $\Delta G^{\#}$ in order to discuss on PCET. The rate constant of the most active compounds (e.g., compound **7**) is ranging from 10^{-1} to 10^{6} M^{-1} s^{-1} (Table 5), probably within an intermediate value. Compounds having only one OH group (**1**–**3**) are 10^3 less active than **7**. Interestingly, BDE correlates with $\Delta G^{\#}$ ($R^2 = 0.99$) when the two most

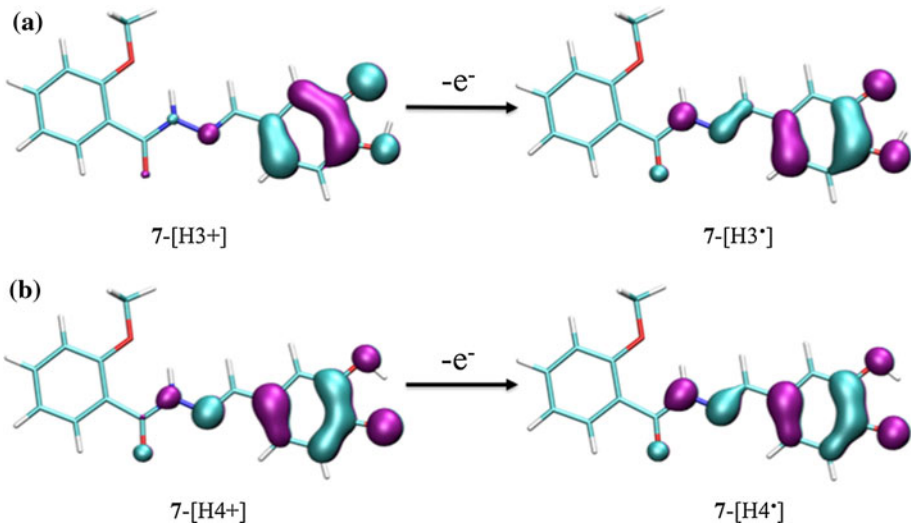

Fig. 5 HOMOs distribution with electron abstraction **a** from **7**-[3H+] to **7**-[3H$^{\cdot}$] and **b** from **7**-[4H+] to **7**-[4H$^{\cdot}$]

active compounds are excluded (Fig. 4). Regarding these two compounds, the intramolecular H-bonding may strongly influence kinetics.

The mechanism of antioxidant activity of polyphenols is known to be dependent on pH [29, 30], due to the capacity of these compounds to deprotonate, leading to an anion having a better capacity to release an electron to the free radical (SPLET mechanism as described in Eqs. 3–5). SPLET is investigated on the most active compound studied here (**7**). In this case, only the two OH groups of the catechol moiety (3-OH and 4-OH) can be deprotonated. From our calculations, the 4-OH group appears slightly more acidic than 3-OH by 2.6 kcal/mol (Table 6); here we quote **7**-[4H+] and **7**-[3H+] the deprotonated form of **7** at C4 and C3, respectively.

As expected, IP of the deprotonated form is lower than that of parent molecule by 1.32 and 1.27 eV for **7**-[3H+] and **7**-[4H+], respectively. No significant difference is observed between the electron donor capacities of **7**-[3H+] and **7**-[4H+] (IP = 4.14 and 4.19 eV, respectively). This highlights that the electron donor capacity of **7** is related to the catechol moiety and not only one specific OH group.

The electron transfer towards the free radical is expected only if a non-covalent pre-reaction complex is formed between the antioxidant and the free radical. Two types of pre-reaction complexes may exist, both involving the O-atom lone pair of the free radical (Fig. 1 in SI). The first type involves a H-bond with the OH group of the antioxidant ([**HB**]-type complex), as observed in the PCET mechanism; the second involves a [***ν*–π**] dispersive interaction with aromatic π-electrons (i.e., [***ν*–π**]-type). It must be stressed that quantum calculations did not allow obtaining [***ν*–π**]-type interactions with N–N π-electrons.

From these pre-reaction complexes, the calculated SPLET rate constants are in the range from 10^{-30} to 10^{-3} M^{-1} s^{-1} (Table 6). These rate constants strongly depend on (1) the electron donor anion (i.e., **7**-[3H+] and **7**-[4H+]) and (2) the geometry of pre-reaction complexes (Fig. 1 in SI). The **7**-[4H+] anion exhibits the highest rate constants (10^{-3} and 10^{-5} M^{-1} s^{-1} for **7**-[3H+] and **7**-[4H+], respectively). Moreover the **7**-[4H+] anion and the subsequent (post-ET) phenoxyl radical (i.e., **7**-[4H˙]) show a better π-conjugation than **7**-[3H+] (Fig. 5). Furthermore, the electronic coupling is significantly different between the reactions of both anions (Table 6). According to V_{RP} formula, the lower the molecular orbital (MO) modification along the reaction, the higher the reactant–product overlap S_{RP}, the higher the electron coupling V_{RP} and therefore the higher the rate constant k^{SPLET}. The highest occupied MO (HOMO) modification from **7**-[4H+] to **7**-[4H˙] is low while HOMOs of **7**-[3H+] and **7**-[3H˙] have the same location but with opposite sign (Fig. 5), highlighting a broken orbital symmetry and thus decreasing the corresponding rate constants.

Compare to quercetin, an antioxidant of reference, the SPLET rate constants are significantly lower. Therefore, the present series of compounds are not expected to be powerful free radical scavenging by ET process, even from the deprotonated (activated) forms. The π-delocalization in the Schiff bases studied here is less extended than in quercetin, thus significantly decreasing the positive energetic contributions (e.g., internal reorganization λ_i, $\Delta G°$) along the electron transfer process.

Conclusion

Based on a series of synthetized Schiff bases, the present study has confirmed the role of the catechol moiety and the importance of the O–H BDE descriptor. Other minor descriptors succeeded in explaining slight differences in antioxidant activity, namely spin density distribution and BDE_d. The latter descriptor elegantly rationalizes the role of the NH group that, according to the chemical structure, may provide a hydrogen atom for a second HAT. Bromine substitution may slightly enhance antioxidant activity. The free radical scavenging capacity of these compounds mainly proceeds by PCET rather than SPLET, the latter mechanism being only feasible at relatively high pH.

Acknowledgments The authors thank the "Conseil Régional du Limousin" for CALI (CAlcul en LImousin) and Atta-ur-Rahman Institute for Natural Product Discovery, Universiti Teknologi for computing facilities. The authors thank the "Pharmacology and Toxicology Research Laboratory-Faculty of Pharmacy, Universiti Teknologi MARA, Puncak Alam Campus, Malaysia" for antioxidant facilities. P.T. gratefully acknowledges the support by the Operational Program Research and Development for Innovations–European Regional Development Fund (project CZ.1.05/2.1.00/03.0058 of the Ministry of Education, Youth and Sports of the Czech Republic). I.B. and P.T. gratefully thank the 'Association Djerbienne de France' (ADF) for the financial support.

References

1. Rice-Evans C, Miller NJ, Paganga G (1996) Structure–antioxidant activity relationships of flavonoids and phenolic acids. Free Radic Biol Med 20:933–956
2. Halliwell B, Aeschbach R, Löliger J, Aruoma OI (1995) The characterization of antioxidants. Food Chem Toxicol 33:601–617
3. Anouar E, Calliste C, Kosinova P, Di Meo F, Duroux J, Champavier Y, Marakchi K, Trouillas P (2009) Free radical scavenging properties of guaiacol oligomers: a combined experimental and quantum study of the guaiacyl-moiety role. J Phys Chem A 113:13881–13891
4. Vicini P, Geronikaki A, Incerti M, Busonera B, Poni G, Cabras CA, La Colla P (2003) Synthesis and biological evaluation of benzo [*d*] isothiazole, benzothiazole and thiazole Schiff bases. Bioorg Med Chem 11:4785–4789

5. Tarafder M, Kasbollah A, Saravanan N, Crouse KA, Ali AM (2002) S-methyldithiocarbazate and its Schiff bases: evaluation of bondings and biological properties. J Biochem Mol Biol Biophys 6:85–91
6. Khan KM, Ahmad A, Ambreen N, Amyn A, Perveen S, Khan SA, Choudhary MI (2009) Schiff bases of 3-formylchromones as antibacterial, antifungal, and phytotoxic agents. Lett Drug Des Discov 6:363–373
7. Chohan ZH, Pervez H, Rauf A, Khan KM, Supuran CT (2006) Antibacterial cobalt (II), copper (II), nickel (II) and zinc (II) complexes of mercaptothiadiazole-derived furanyl, thienyl, pyrrolyl, salicylyl and pyridinyl Schiff bases. J Enzyme Inhib Med Chem 21:193–201
8. Chohan ZH, Pervez H, Rauf A, Khan KM, Maharvi GM, Supuran CT (2004) Antibacterial and antifungal mono-and di-substituted symmetrical and unsymmetrical triazine-derived Schiff-bases and their transition metal complexes. J Enzyme Inhib Med Chem 19:161–168
9. Kabeer AS, Baseer M, Mote N (2001) Synthesis and antimicrobial activity of some Schiff bases from benzothiazoles. Asian J Chem 13:496–500
10. Chohan ZH, Arif M, Shafiq Z, Yaqub M, Supuran CT (2006) In vitro antibacterial, antifungal & cytotoxic activity of some isonicotinoylhydrazide Schiff's bases and their cobalt (II), copper (II), nickel (II) and zinc (II) complexes. J Enzyme Inhib Med Chem 21:95–103
11. Guo Z, Xing R, Liu S, Zhong Z, Ji X, Wang L, Li P (2007) Antifungal properties of Schiff bases of chitosan, N-substituted chitosan and quaternized chitosan. Carbohydr Res 342:1329–1332
12. Taha M, Baharudin MS, Ismail NH, Khan KM, Jaafar FM, Siddiqui S, Iqbal Choudhary M (2013) Synthesis of 2-methoxybenzoylhydrazone and evaluation of their antileishmanial activity. Bioorg Med Chem Lett 23:3463–3466
13. Mohammed Khan K, Taha M, Naz F, Siddiqui S, Ali S, Rahim F, Perveen S, Iqbal Choudhary M (2012) Acylhydrazide Schiff bases: DPPH radical and superoxide anion scavengers. Med Chem 8:705–710
14. Mohammed Khan K, Shah Z, Uddin Ahmad V, Khan M, Taha M, Rahim F, Ali S, Ambreen N, Perveen S, Iqbal Choudhary M (2012) 2,4,6-Trichlorophenylhydrazine Schiff bases as DPPH radical and super oxide anion scavengers. Med Chem 8:452–461
15. Trouillas P, Marsal P, Siri D, Lazzaroni R, Duroux J-L (2006) A DFT study of the reactivity of OH groups in quercetin and taxifolin antioxidants: the specificity of the 3-OH site. Food Chem 97:679–688
16. Kozlowski D, Trouillas P, Calliste C, Marsal P, Lazzaroni R, Duroux J-L (2007) Density functional theory study of the conformational, electronic, and antioxidant properties of natural chalcones. J Phys Chem A 111:1138–1145
17. Leopoldini M, Russo N, Toscano M (2011) The molecular basis of working mechanism of natural polyphenolic antioxidants. Food Chem 125:288–306
18. Wang L-F, Zhang H-Y (2003) A theoretical investigation on DPPH radical-scavenging mechanism of edaravone. Bioorg Med Chem Lett 13:3789–3792
19. Netto LE, Chae HZ, Kang S-W, Rhee SG, Stadtman ER (1996) Removal of hydrogen peroxide by thiol-specific antioxidant enzyme (TSA) is involved with its antioxidant properties TSA possesses thiol peroxidase activity. J Biol Chem 271:15315–15321
20. Halliwell B (1991) Reactive oxygen species in living systems: source, biochemistry, and role in human disease. Am J Med 91:S14–S22
21. Di Mascio P, Murphy ME, Sies H (1991) Antioxidant defense systems: the role of carotenoids, tocopherols, and thiols. Am J Clin Nutr 53:194S–200S
22. Saito H, Ishihara K (1997) Antioxidant activity and active sites of phospholipids as antioxidants. J Am Oil Chem Soc 74:1531–1536
23. Padmaja A, Rajasekhar C, Muralikrishna A, Padmavathi V (2011) Synthesis and antioxidant activity of oxazolyl/thiazolylsulfonylmethyl pyrazoles and isoxazoles. Eur J Med Chem 46:5034–5038
24. Brede O, Ganapathi MR, Naumov S, Naumann W, Hermann R (2001) Localized electron transfer in nonpolar solution: reaction of phenols and thiophenols with free solvent radical cations. J Phys Chem A 105:3757–3764
25. DiLabio GA, Johnson ER (2007) Lone pair-π and π–π interactions play an important role in proton-coupled electron transfer reactions. J Am Chem Soc 129:6199–6203
26. Hatcher E, Soudackov AV, Hammes-Schiffer S (2007) Proton-coupled electron transfer in soybean lipoxygenase: dynamical behavior and temperature dependence of kinetic isotope effects. J Am Chem Soc 129:187–196
27. Hammes-Schiffer S (2012) Proton-coupled electron transfer: classification scheme and guide to theoretical methods. Energy Environ Sci 5:7696–7703
28. Lingwood M, Hammond JR, Hrovat DA, Mayer JM, Borden WT (2006) MPW1 K performs much better than B3LYP in DFT calculations on reactions that proceed by proton-coupled electron transfer (PCET). J Chem Theory Comput 2:740–745
29. Di Meo F, Lemaur V, Cornil J, Lazzaroni R, Duroux J-L, Olivier Y, Trouillas P (2013) Free radical scavenging by natural polyphenols: atom versus electron transfer. J Phys Chem A 117:2082–2092
30. Musialik M, Kuzmicz R, Pawlowski Tomasz S, Litwinienko G (2009) Acidity of hydroxyl groups: an overlooked influence on antiradical properties of flavonoids. J Org Chem 74:2699–2709
31. Trouillas P, Marsal P, Svobodova A, Vostalova J, Gazak R, Hrbac J, Sedmera P, Kren V, Lazzaroni R, Duroux J-L, Walterova D (2008) Mechanism of the antioxidant action of silybin and 2,3-dehydrosilybin flavonolignans: a joint experimental and theoretical study. J Phys Chem A 112:1054–1063
32. Iuga C, Alvarez-Idaboy JRl, Russo N (2012) Antioxidant activity of trans-resveratrol toward hydroxyl and hydroperoxyl radicals: a quantum chemical and computational kinetics study. J Org Chem 77:3868–3877
33. Leopoldini M, Chiodo SG, Russo N, Toscano M (2011) Detailed investigation of the OH radical quenching by natural antioxidant caffeic acid studied by quantum mechanical models. J Chem Theory Comput 7:4218–4233
34. Alberto ME, Russo N, Grand A, Galano A (2013) A physicochemical examination of the free radical scavenging activity of Trolox: mechanism, kinetics and influence of the environment. Phys Chem Chem Phys 15:4642–4650
35. Blois MS (1958) Antioxidant determinations by the use of a stable free radical. Nature 181:1199–1200
36. Frisch MJ et al (2009) Gaussian 09, Revision A.02. Gaussian, Inc., Wallingford, CT
37. Anouar EH, Gierschner J, Duroux J-L, Trouillas P (2012) UV/Visible spectra of natural polyphenols: a time-dependent density functional theory study. Food Chem 131:79–89
38. Košinová P, Di Meo F, Anouar EH, Duroux JL, Trouillas P (2011) H-atom acceptor capacity of free radicals used in antioxidant measurements. Int J Quantum Chem 111:1131–1142
39. Chiodo SG, Leopoldini M, Russo N, Toscano M (2010) The inactivation of lipid peroxide radical by quercetin. A theoretical insight. Phys Chem Chem Phys 12:7662–7670
40. Zhao Y, Truhlar DG (2004) Hybrid meta density functional theory methods for thermochemistry, thermochemical kinetics, and noncovalent interactions: the MPW1B95 and MPWB1K models and comparative assessments for hydrogen bonding and van der Waals interactions. J Phys Chem A 108:6908–6918

41. Tejero I, González-García N, González-Lafont À, Lluch JM (2007) Tunneling in green tea: understanding the antioxidant activity of catechol-containing compounds. A variational transition-state theory study. J Am Chem Soc 129:5846–5854
42. Tomasi J, Mennucci B, Cammi R (2005) Quantum mechanical continuum solvation models. Chem Rev 105:2999–3093
43. Guerra M, Amorati R, Pedulli GF (2004) Water effect on the OH dissociation enthalpy of para-substituted phenols: a DFT study. J Org Chem 69:5460–5467
44. Farazdel A, Dupuis M, Clementi E, Aviram A (1990) Electric-field induced intramolecular electron transfer in spiro.pi.-electron systems and their suitability as molecular electronic devices. A theoretical study. J Am Chem Soc 112:4206–4214
45. Grimme S (2004) Accurate description of van der Waals complexes by density functional theory including empirical corrections. J Comput Chem 25:1463–1473
46. Grimme S (2006) Semiempirical GGA-type density functional constructed with a long-range dispersion correction. J Comput Chem 27:1787–1799
47. Grimme S, Antony J, Ehrlich S, Krieg H (2010) A consistent and accurate ab initio parametrization of density functional dispersion correction (DFT-D) for the 94 elements H-Pu. J Chem Phys 132:154104–154123
48. Di Meo F, Sancho Garcia JC, Dangles O, Trouillas P (2012) Highlights on anthocyanin pigmentation and copigmentation: a matter of flavonoid π-stacking complexation to be described by DFT-D. J Chem Theory Comput 8:2034–2043
49. Neese F (2012) The ORCA program system. Wiley Interdiscip Rev Comput Mol Sci 2:73–78
50. Valiev M, Bylaska EJ, Govind N, Kowalski K, Straatsma TP, Van Dam HJJ, Wang D, Nieplocha J, Apra E, Windus TL, de Jong WA (2010) NWChem: a comprehensive and scalable open-source solution for large scale molecular simulations. Comput Phys Commun 181:1477–1489
51. Neese F, Wennmohs F, Hansen A, Becker U (2009) Efficient, approximate and parallel Hartree-Fock and hybrid DFT calculations. A 'chain-of-spheres' algorithm for the Hartree-Fock exchange. Chem Phys 356:98–109
52. Mahoney LR, Mendenhall GD, Ingold KU (1973) Calorimetric and equilibrium studies on some stable nitroxide and iminoxy radicals. Approximate oxygen-hydrogen bond dissociation energies in hydroxylamines and oximes. J Am Chem Soc 95:8610–8614